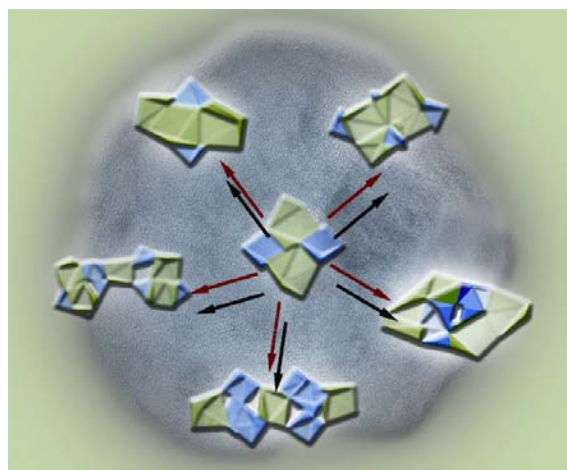
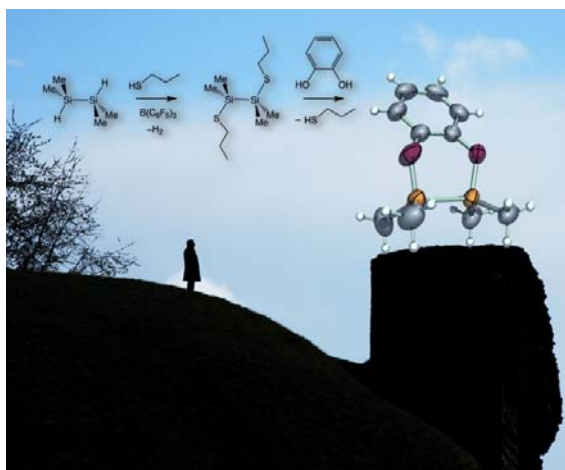


This paper is published as part of a *Dalton Transactions* theme issue on:

Main group chemistry: from molecules to materials

Guest Editor Simon Aldridge
University of Oxford, UK

Published in [issue 26, 2008](#) of *Dalton Transactions*



Images reproduced with permission of Daniel M. German (left) and Vadim Kessler (right)

Papers published in this issue include:

[Heteroleptic metal alkoxide “oxoclusters” as molecular models for the sol–gel synthesis of perovskite nanoparticles for bio-imaging applications](#)

Gulaim A. Seisenbaeva, Vadim G. Kessler, Robert Pazik and Wieslaw Streck, *Dalton Trans.*, 2008, DOI: [10.1039/b801351a](#)

[Hydride encapsulation by molecular alkali-metal clusters](#)

Joanna Haywood and Andrew E. H. Wheatley, *Dalton Trans.*, 2008, DOI: [10.1039/b717563a](#)

[Manipulation of molecular aggregation and supramolecular structure using self-assembled lithium mixed-anion complexes](#)

J. Jacob Morris, Dugald J. MacDougall, Bruce C. Noll and Kenneth W. Henderson, *Dalton Trans.*, 2008, DOI: [10.1039/b719565f](#)

[Toward selective functionalisation of oligosilanes: borane-catalysed dehydrogenative coupling of silanes with thiols](#)

Daniel J. Harrison, David R. Edwards, Robert McDonald and Lisa Rosenberg, *Dalton Trans.*, 2008, DOI: [10.1039/b806270f](#)

Visit the *Dalton Transactions* website for more cutting-edge inorganic and organometallic research
www.rsc.org/dalton

Electronic structure of the glyoxalbis(2-hydroxyanil) (gha) ligand in $[\text{Co}^{\text{III}}(\text{gha})(\text{PPh}_3)_2]^+$: radical vs. non-radical states†

Amit Saha Roy,^a Nicoleta Muresan,^b Heikki M. Tuononen,^c Sankar P. Rath^d and Prasanta Ghosh^{*a}

Received 5th February 2008, Accepted 20th May 2008

First published as an Advance Article on the web 9th June 2008

DOI: 10.1039/b802063a

The synthesis, structure and spectroscopic properties of a complex salt $[\text{Co}^{\text{III}}(\text{gha})(\text{PPh}_3)_2][\text{Co}^{\text{II}}\text{Cl}_3(\text{PPh}_3)] \cdot \text{C}_2\text{H}_5\text{OH}$ (**1**) are reported; gha = glyoxalbis(2-hydroxyanil). This is the first single crystal X-ray structure of a $(\text{gha})^{2-}$ complex with a transition element. Though the determined bond parameters and UV-Vis spectroscopic data correlate well with a diradical description for the cation in **1**, detailed electronic structure calculations using density functional theory confirm that $[\text{Co}(\text{gha})(\text{PPh}_3)_2]^+$ can be described as a closed shell singlet species which nevertheless displays an interesting electronic structure with significant electron transfer to the formally unoccupied LUMO of the square planar $[\text{Co}(\text{gha})]^+$ fragment. It was found that without the phosphine coligands, the $[\text{Co}(\text{gha})]^+$ unit has a triplet ground state with the lowest energy singlet diradical state lying only 1 kcal mol⁻¹ higher in energy. The chemistry of the gha ligand is of interest as a spin diverse redox active system.

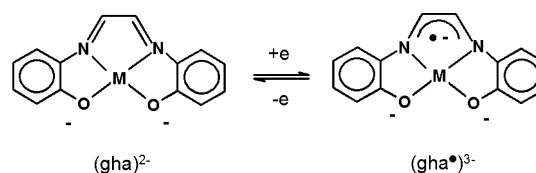
Introduction

Ever since Gomberg's discovery of the triphenylmethyl radical at the turn of the 20th century,¹ stable radicals have fascinated researchers. This has led to isolation and characterization of an ever-increasing number of stable and persistent odd-electron species of the main group elements.² Quintessential examples are the thiazyl,^{2c,3} verdazyl^{2c,4} and nitroxide radical families,^{2c,5} to name a few. From a fundamental perspective, the study of these systems is of importance because they not only challenge our conventional chemical thinking, but also develop our understanding of molecular structure and bonding. In addition, the paramagnetic nature of stable radicals renders them useful in many applications: among other things, radicals can be used as polymerization catalysis,⁶ reagents in redox chemistry⁷ and as building blocks for molecule-based materials.⁸

As can be expected, not all radicals are stable in their own right. Fortunately stabilization can in many cases be achieved *via* coordination of the paramagnetic species to metal centers. The spectroscopic and structural studies of the properties and reactivities of such systems have become particularly important in exploring many chemical and biological reactions in detail.⁹ For example, the bond parameters and the spectral features of benzosemiquinone,^{9d,10} iminobenzosemiquinone,¹¹

diiminobenzosemiquinone,¹² iminothiobenzosemiquinone¹³ and the more reactive phenoxyl,¹⁴ anilino,¹⁵ aminyl,¹⁶ thiyyl¹⁷ and azo-anion¹⁸ radicals are now well established. To stabilize new organic mono- and polyradicals as coordination complexes with one or multiple paramagnetic sites in one molecule is an ongoing challenge in modern radicals research.

Recently it has been recognized that the dianion of *cis*-glyoxalbis(2-mercaptoanil) (*cis*-gma), a tetradentate ligand, is redox active. Its diimine fragment can be reduced by one electron to form a monoradical trianionic ligand, (*cis*-gma^{•3-}), which has been experimentally characterized as an iron coordinated species.¹⁹ Coordination of the novel excited triplet state of (*cis*-gma)²⁻ has also been evidenced in $[\text{Fe}(\text{gma})(\text{X})]^n$ (X = pyridine, $n = 1+$; X = CN⁻, I⁻, $n = 0$).¹⁹ As a possibility to extend the chemistry of stable organic radical ligands further, the oxygen analogue of *cis*-gma, the *cis*-glyoxalbis(2-hydroxyanil) (*cis*-gha) ligand, is of immediate interest.²⁰ The coordination chemistry of *cis*-gha has so far been established in tetradentate dianionic form, (*cis*-gha)²⁻,²¹ in *trans* conformation, *cis*-gha functions as a noninnocent bis-bidentate bridging ligand.²² However, *cis*-gha can potentially bind a metal centre also as an open shell trianionic π -radical, (gha^{•3-}), in which the unpaired electron becomes localized on the diimine moiety (Scheme 1). Parallel behavior has been observed for the (*trans*-gha)²⁻ ligand in its diruthenium^{III} complex.²²



Scheme 1 Deprotonated dianionic (gha)²⁻ and trianionic (gha^{•3-}) forms of metal coordinated glyoxalbis(2-hydroxyanil).

^aDepartment of Chemistry, R. K. Mission Residential College, Narendrapur, Kolkata, 103, India. E-mail: ghoshp_chem@yahoo.co.in; Fax: 091 33 2477 3597; Tel: 091 33 2428 7017

^bMax-Planck-Institut für Bioorganische Chemie, Stiftstrasse 34-36, D-45470, Mülheim an der Ruhr, Germany

^cDepartment of Chemistry, University of Jyväskylä, P.O. Box 35, FI-40014, Jyväskylä, Finland

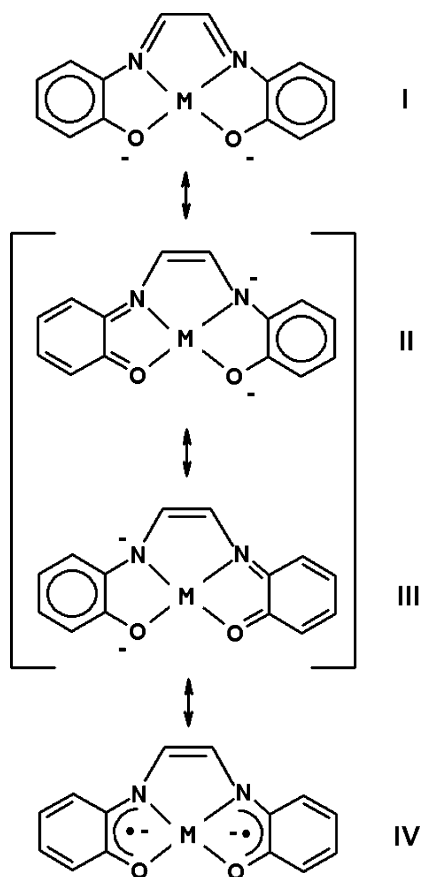
^dDepartment of Chemistry, Indian Institute of Technology, Kanpur, 208016, India

† Electronic supplementary information (ESI) available: Full crystallographic tables of **1** as well as optimized coordinates for $[\text{Co}(\text{gha})]^+$ and $[\text{Co}(\text{gha})(\text{PH}_3)]^+$. CCDC reference number 621602. For crystallographic data in CIF or other electronic format see DOI: 10.1039/b802063a

In order to correctly describe the electronic properties of the gha ligand, or for that matter any other kind of ligand, in its

coordination complexes, it is of critical importance to obtain structural and spectroscopic data of the systems under study. Unfortunately the low solubility of the metal complexes of gha in common non-coordinating solvents is a problem which to some extent thwarts both crystallization and collection of different physicochemical data. In addition, it is in general difficult to explore the coordination chemistry of the gha ligand because it forms an equilibrium with 2,2'-bisbenzoxazoline,^{20e,23} the solubility of which is low and is therefore easily separated out from the reaction mixture. The only published single crystal X-ray structure of a gha complex is for a uranium species aquaglyoxalbis(2-hydroxyanil)dioxouranium, (H₂O)UO₂(gha), and the reported bond parameters do not allow elucidation of the details of the electronic structure within the dianionic ligand.^{21a,21c} The scarcity of fully characterized (including single crystal X-ray data) transition metal compounds containing the gha ligand has not allowed the detailed determination of its electronic structure till date though the ligand itself has been reported as early as 1950s.²⁰

The electronic structure of the (*cis*-gha)²⁻ ligand can be adequately described using the resonance structure **I** containing two phenolato-type ions (see Scheme 2). However, depending on the metal fragment to which the ligand binds to, the significance of other resonance structures can increase considerably. The inclusion of closed shell resonance structures **II** and **III** to the description in Scheme 2 emphasizes this by incorporating one neutral quinone-type ring and another dianionic catecholato-type ring in one molecule, thus, delocalizing the formal charge from oxygen to nitrogen atoms. However, since the (gha)²⁻ ligand is



Scheme 2 Possible resonance structures for the (gha)²⁻ ligand.

known to be redox active, the description should be augmented also with radical-type resonance structures alike **IV** as their importance cannot be neglected *a priori*.

We have now synthesized a (*cis*-gha)²⁻ complex in which the tetradentate dianionic ligand is coordinated to an octahedral cobalt(III) ion in a salt [Co^{III}(gha)(PPh₃)₂][Co^{II}Cl₃(PPh₃)₂·C₂H₅OH (**1**). The structural and electronic properties of the complex were studied *via* different experimental methods *i.e.* X-ray crystallography, spectroscopy, electrochemistry and magnetochemistry. In addition, we have used density functional theory (DFT) in order to rationalize the bonding and spectroscopic properties of [Co(gha)(PPh₃)₂]⁺. Compound **1** represents the first single crystal X-ray structure of a (gha)²⁻ complex with a d-block element. The collected experimental and computational data indicates that in the cation of **1**, the (*cis*-gha)²⁻ ligand adopts a different electronic configuration depending on the coordination sphere of the Co^{III} center: a truncated model system [Co(gha)]⁺ represents a chemical species in which the gha ligand coordinates to a metal using an open shell diradical singlet state (**IV** in Scheme 2), whereas a closed shell singlet configuration is observed for the ligand in [Co(gha)(PPh₃)₂]⁺. However, the structural and spectral data determined for the cation of **1** indicates that its electronic structure is phenoxyl rather than phenolato-type, reminiscent of the diradical character calculated for [Co(gha)]⁺.

Experimental

Synthesis

[Co^{III}(gha)(PPh₃)₂][Co^{II}Cl₃(PPh₃)₂·C₂H₅OH (**1**). To a 30% aqueous solution of glyoxal (1 mmol) in absolute ethanol (30 ml) and acetonitrile (5 ml), 2-hydroxyaniline (220 mg, 2 mmol) was added and the reaction mixture refluxed for 40 min after which the solution turned yellowish-brown. To this hot solution, anhydrous CoCl₂ (260 mg, 2 mmol) and triphenylphosphine (1050 mg, 4 mmol) were added successively and the mixture refluxed gently for further 60 min. The dark green solution was filtered hot and the colored filtrate was cooled at room temperature and allowed to evaporate slowly in air. Within two days, dark green needles of **1** separated out. Yield: 700 mg (56% with respect to Co). Elemental anal. (%) for C₆₈H₅₅N₂O₂P₃Cl₃Co₂·C₂H₅OH: Calcd. C 64.91, H 4.67, N 2.16; Found C 64.60, H 4.45, N 2.05. ESI MS: *m/z*, 821.2 [Co(gha)(PPh₃)₂]⁺, 425.5 [CoCl₃(PPh₃)₂]⁻. IR(KBr) (cm⁻¹): 1585(w), 1509(s), 1435(vs), 1093(s), 694(vs), 519(vs).

X-Ray crystallographic data collection and refinement of the structure

Single crystal X-ray data† were collected at -173 °C on a Bruker SMART APEX CCD diffractometer using graphite-monochromatic Mo K α radiation ($\lambda = 0.71073$ Å). The linear absorption coefficients, scattering factors for the atoms and the anomalous dispersion corrections were taken from International Tables for X-Ray Crystallography. The data integration and reduction were processed with SAINT software.²⁴ An absorption correction was applied.²⁵ The structure was solved by direct methods using SHELXS-97 and was refined on *F*² by full-matrix least-squares technique using the SHELXL-97 program package.²⁶ All the non-hydrogen atoms of the molecule were

Table 1 Crystallographic data for $[\text{Co}(\text{gha})(\text{PPh}_3)_2][\text{CoCl}_3(\text{PPh}_3)] \cdot \text{C}_2\text{H}_5\text{OH}$ (**1**)

Chemical formula	$\text{C}_{68}\text{H}_{55}\text{N}_2\text{O}_2\text{P}_3\text{Cl}_3\text{Co}_2 \cdot \text{C}_2\text{H}_5\text{OH}$
FW	1295.32
Crystal system	Monoclinic
Space group	$P2_1/n$
$a/\text{\AA}$	15.4277(15)
$b/\text{\AA}$	11.4944(11)
$c/\text{\AA}$	34.924(4)
$\beta/^\circ$	101.703(2)
$V/\text{\AA}^3$	6064.5(10)
Z	4
T/K	100(2)
$\rho_{\text{calcd}}/\text{g cm}^{-3}$	1.419
Reflections collected	14481
$R(\text{int})$	0.1126
Unique reflections; $I > 2\sigma(I)$	14481; 6618
No. of parameters	749
$\lambda/\text{\AA}; \mu(\text{Mo K}\alpha)/\text{mm}^{-1}$	0.71073; 0.809
$R1^a$; goodness of fit ^b	0.0718; 0.874
$wR2^c [I > 2\sigma(I)]$	0.1306
Residual density/ $e \text{\AA}^{-3}$	0.914

^a Observation criterion: $I > 2\sigma(I)$. $R1 = \sum \|F_o\| - |F_c| / \sum \|F_o\|$. ^b GOF = $[\sum [w(F_o^2 - F_c^2)^2] / (n - p)]^{1/2}$. ^c $wR2 = [\sum [w(F_o^2 - F_c^2)^2] / \sum [w(F_o^2)^2]]^{1/2}$ where $w = 1/\sigma^2(F_o^2) + (ap)^2 + bP$, $P = (F_o^2 + 2F_c^2)/3$.

refined anisotropically. The C–O bond length and C–C–O angle of the ethanol are restrained to sensible values. In the refinement, hydrogen atoms were treated as riding atoms using SHELXL default parameters. Crystallographic data of compound **1** are listed in Table 1.

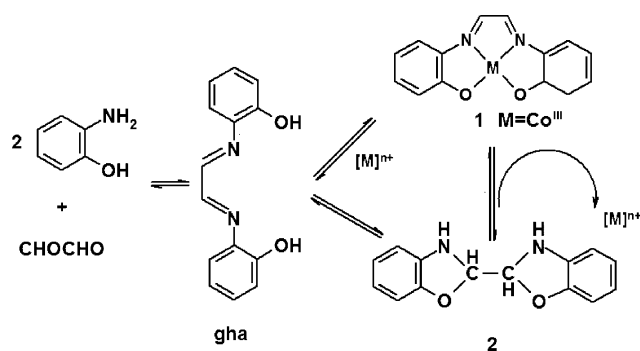
Density functional theory calculations

We performed the theoretical calculations of this paper using the Turbomole and ORCA program packages.²⁷ The geometry optimizations were carried out at the BP86 level.²⁸ The Gaussian basis sets were those reported by the Ahlrichs group.²⁹ Triple- ζ quality basis sets with one set of polarization functions on the cobalt, oxygen, nitrogen and phosphorus atoms were used (TZVP).^{29b} The carbon and hydrogen atoms were described by slightly smaller polarized split-valence SV(P) basis sets that is double- ζ quality in the valence region and contains a polarizing set of d-functions on the non-hydrogen atoms.^{29a} The auxiliary basis sets for all complexes used to expand the electron density in the calculations were chosen to match the orbital basis. Fragment orbital analysis for $[\text{Co}(\text{gha})(\text{PH}_3)_2]^+$ was performed with the ADF program using the PB86 density functional with TZP quality STO basis sets.³⁰ Orbital and density plots were obtained by the program gOpenMol.³¹

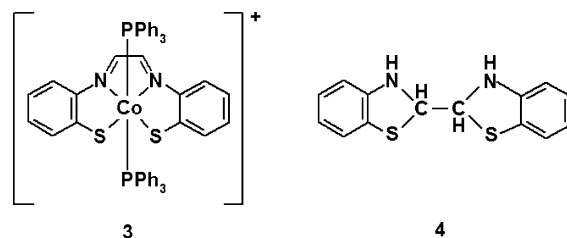
Results and discussion

Synthesis

We have been interested in isolating complexes containing the $(\text{gha})^{2-}$ ligand for physicochemical measurements in order to establish the potential of this system to act as a spin diverse ligand in its coordination compounds. However, all our previous attempts failed to afford a binary compound of gha with a 3d metal. It has been established that in every case 2,2'-bisbenzooxazoline (**2**) separates out from the reaction mixture (see Scheme 3).

**Scheme 3** Synthesis of **1**.

To slightly modify the synthetic approach in Scheme 3, we decided to see what effect, if any, the introduction of coligands (**L**) to the reaction mixture would have. It was hoped that by approaching a higher coordination at the metal centre, the desired metal complex would crystallize out from the reaction mixture. So far the chosen approach has been the most successful when $M = \text{Co}$ and when PPh_3 acts as a coligand, separating out the complex salt **1**. We note that similar reactions employing various other 3d metal ions did not yield any crystalline products.



Interestingly, the reaction of 2-mercaptoaniline and glyoxal with Co under similar reaction conditions does not yield a cation of the type **3** containing the $(\text{gma})^{2-}$ ligand but furnishes only 2,2'-bisbenzothiooxazoline (**4**). The increased reactivity of the dioxygen species in contrast to its heavier sulfur analogue is encouraging but the degradation of **1** to **2** in solution is nevertheless found to be rapid. Hence, the transformation of gha and gma to the more stable oxazoline **2** and thiooxazoline **4**, respectively, is the limiting factor for the development of coordination chemistry of these ligands. Only a very specific combination of transition metal cations and coligands seems to be effective in stabilizing **1** so that it can be crystallized.

X-Ray structure

The compound **1** has been isolated as dark green crystals from which single crystals for X-ray structure determination have been collected. The complex **1** crystallizes in $P2_1/n$ space group. Fig. 1 displays the structure of **1** determined at 100 K.

In the cation of **1**, the Co(1) center is octahedrally coordinated to a tetradentate dianionic gha ligand and to two monodentate triphenylphosphine coligands. In the anion, the Co(2) center is tetrahedrally coordinated by three chloride ions and one triphenylphosphine ligand. The average Co(1)–P bond distance (2.308 Å) is shorter than the Co(2)–P(3) distance (2.401 Å) by approximately 0.10 Å reflecting the different geometry and formal oxidation state of the two cobalt centers in **1** (+III and +II in the cation and the anion, respectively).

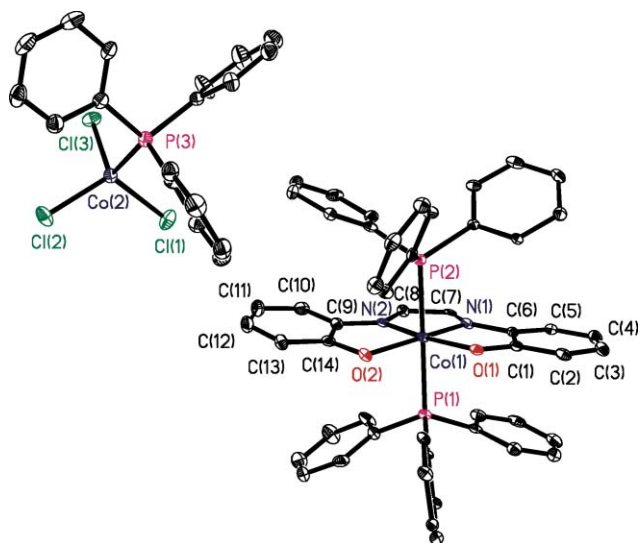


Fig. 1 X-Ray single crystal structure of **1**. The solvent molecule C_2H_5OH and hydrogen atoms are omitted for clarity. Key bond lengths (\AA) and angles ($^\circ$): Co(1)–O(1) 1.934(3), Co(1)–O(2) 1.948(3), Co(1)–N(1) 1.852(4), Co(1)–N(2) 1.855(4), Co(1)–P(1) 2.2737(15), Co(1)–P(2) 2.3435(15), O(1)–C(1) 1.314(6), O(2)–C(14) 1.333(5), N(1)–C(6) 1.382(6), N(1)–C(7) 1.306(5), N(2)–C(8) 1.321(6), N(2)–C(9) 1.386(6), C(7)–C(8) 1.417(6); N(1)–Co(1)–N(2) 83.58(18), N(1)–Co(1)–O(1) 85.31(16), N(2)–Co(1)–O(1), 168.88(17), N(1)–Co(1)–O(2) 167.69(15), N(2)–Co(1)–O(2) 85.20(16), O(1)–Co(1)–O(2) 105.91(14), P(1)–Co(1)–P(2) 169.93(6); Co(2)–Cl(1) 2.2677(17), Co(2)–Cl(2) 2.2262(17), Co(2)–Cl(3) 2.2313(15), Co(2)–P(3) 2.4016(16), Cl(2)–Co(2)–Cl(3) 110.48(7), Cl(2)–Co(2)–Cl(1) 114.20(7), Cl(3)–Co(2)–Cl(1) 109.45(6), Cl(3)–Co(2)–P(3) 108.00(6), Cl(2)–Co(2)–P(3) 108.48(6).

The bond distances in the glyoxal bridging unit of the (gha) $^{2-}$ ligand in **1** are significant in establishing its electronic configuration. In general, the C–C and C–N distances in a neutral diimine are sharply different from those in a corresponding anionic radical which arises from the occupation of the CC-bonding CN-antibonding LUMO by an unpaired electron in the latter species. Single crystal X-ray structure of the paramagnetic spirocyclic Li(1,4-di-*tert*-butyl-1,4-diazabutadiene) $_2$ ($S = 1/2$) has established the feature unequivocally: 32 the C–N and C–C distances in the neutral diimine are 1.24 and 1.49 \AA respectively, whereas the corresponding bond lengths in the diimine anion radical are 1.32 and 1.40 \AA . A similar trend has also been established in the Fe(gma *) species. 19 Interestingly, the bond parameters of the glyoxal fragment in **1** do not support the presence of a diimine (resonance structure **I** in Scheme 2). We also note that the complex **1** exhibits a $\nu_{C=N}$ stretching frequency at 1508 cm^{-1} which is much less than the stretching frequency of a coordinated aldimine function ($> 1600 \text{ cm}^{-1}$) 33 favouring lower bond order of the $\nu_{C=N}$ -group.

In **1**, the C(7)–C(8) length, 1.417(6) \AA , is the average of C(sp 2)–C(sp 2) single (1.49 \AA) and double (1.33 \AA) bonds, and, thus, indicates that the bonding description is either in between the two extremes shown in resonance structures **I** and **II–IV**, or the [Co(gha)(PPh $_3$) $_2$] $^+$ cation contains a diimine anion radical moiety. The latter possibility would imply the presence of a Co IV center which would be atypical oxidation state for cobalt, and is shown to be incorrect description by both structural data as well as results from electronic structure calculations (see below). Similarly to

the C–C bond, the mean C–N bond length in **1**, 1.314 \AA , is intermediate of C(sp 2)–N(sp 2) single and double bonds which further emphasizes the diminished role played by the resonance structure **I** to the description of bonding in **1**.

The metrical parameters of the dianionic gha ligand show a quinoid-type distortion in the two aromatic phenolic rings A and B (see Fig. 2). In the ring A, the average of C(2)–C(3) and C(4)–C(5) bond distances, 1.372 \AA , is shorter than the average bond distance of C(1)–C(2), C(3)–C(4), C(5)–C(6) and C(1)–C(6), 1.412 \AA . The same trend is also evident in the ring B in which both the C(10)–C(11) and C(12)–C(13) bonds are shorter than any of the other ones. The C–O distances also correlate well with this description: the C(1)–O(1), and C(14)–O(2) bond lengths are shorter than C–O bonds in reported cobalt phenolato complexes. 34 It is also noteworthy that both the Co(1)–O(1) and Co(1)–O(2) bond lengths are *ca.* 0.05 \AA longer than the average Co–O distance ($1.89 \pm 0.01 \text{ \AA}$) in the reported phenolato systems. 34 A similar length trend has already been established in a structurally characterized phenoxy radical complex of chromium: 35 the Cr–O distance in the phenoxy system was found to be 1.943(2) \AA while the same bond length is only 1.920(2) \AA in the phenolato analogue. Taken as a whole, the above structural features lend strong support for the importance of resonance structures **II**, **III** and, possibly, the radical-type structure **IV** over **I** to describe the bonding in the cation of **1**.

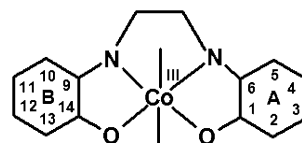


Fig. 2 C–C bond distances (\AA) in the (gha) $^{2-}$ ligand in **1**: C(1)–C(2) 1.410(7), C(2)–C(3) 1.364(7), C(3)–C(4) 1.417(7), C(4)–C(5) 1.379(6), C(5)–C(6) 1.406(7), C(1)–C(6) 1.414(7), C(9)–C(10) 1.393(7), C(10)–C(11) 1.377(7), C(11)–C(12) 1.395(7), C(12)–C(13) 1.368(7), C(13)–C(14) 1.410(7), C(9)–C(14) 1.396(7).

Electronic spectra

The electronic (UV-Vis) spectra of phenoxy radicals are highly characteristic. It has been established that when coordinated to a metal ions, the phenoxy radicals absorb strongly in the ultraviolet part of the spectrum (π – π^* transitions around 400 and $< 300 \text{ nm}$) and only a weak broad transition maximum (ligand-to-metal charge transfer) is observed at around 600–700 nm. 14,36 For the free phenoxy radical, the origin of the π – π^* transitions involving low-lying excited electronic states (2A_2 , 2B_1 , 2A_2 and 2B_1) has been determined using a combination of spectroscopic methods and time-dependent density functional theory. 37 Most importantly, the intense band at around $400 \pm 20 \text{ nm}$ is highly indicative of phenoxy radical formation as analogous phenolato complexes show no absorption at that region. 14,37

Fig. 3 shows the electronic spectrum of **1** in CH_2Cl_2 at 20 $^\circ\text{C}$. The absorption maxima, λ_{max} ($\epsilon/M^{-1} \text{ cm}^{-1}$), occur at 720 (8320), 605 (3790), 410 (19890), 348 (26830) and 250 nm (47410), which indicates that the electronic structure of the ligand in the cation of **1** is closer to phenoxy rather than phenolato in agreement with the conclusions drawn from structural parameters.

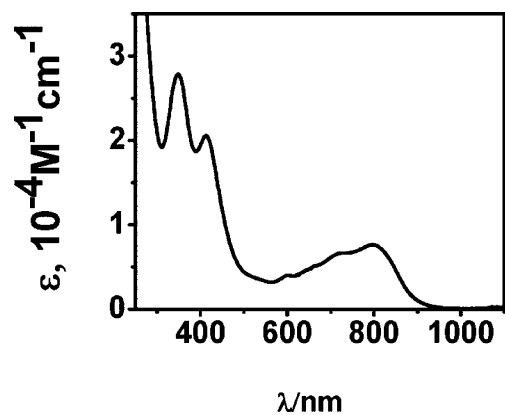


Fig. 3 Electronic spectra of **1** in CH_2Cl_2 at 20°C .

Magnetic measurements

The compound **1** is paramagnetic with $S = 3/2$ ground state as established *via* temperature-dependent (4–290 K) magnetic susceptibility measurements (Fig. 4). The cobalt^{III} ion in the tetrahedral $[\text{CoCl}_3(\text{PPh}_3)]^-$ anion is high-spin with three unpaired electrons ($S = 3/2$ spin state). Consequently, the cation $[\text{Co}(\text{gha})(\text{PPh}_3)_2]^+$ is necessarily diamagnetic which at first glance implies the coordination of singlet state dianionic gha ligand ($S = 0$) to a low-spin octahedral cobalt^{III} ion (t_{2g}^6 configuration). However, both the metrical parameters as well as the UV-Vis spectroscopic data indicate that the electronic structure of the (gha)²⁻ ligand in **1** is of phenoxyl-type *i.e.* it shows diradical-like behavior in which the “unpaired” electron density is not localized on the diimine moiety but on the OCCN chelating fragments (structure **IV** in Scheme 2). In order to correctly identify the complex electronic features of the cation in **1**, it is therefore of

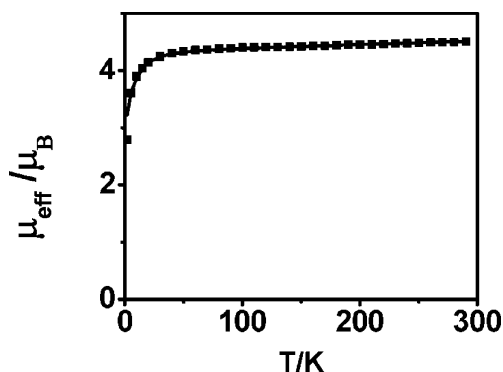


Fig. 4 Temperature dependence of the magnetic moment of a solid sample of **1**. The solid line represents the best fit to the data obtained by using $S = 3/2$ spin state, $g = 2.238$ and $D = 13.5 \text{ cm}^{-1}$.

critical importance to connect the experimental data to theoretical predictions. In the next two sections, a detailed picture of the electronic structure of $[\text{Co}(\text{gha})(\text{PPh}_3)_2]^+$ is given on the basis of results from comprehensive DFT calculations.

The calculated geometries[†] of the monocations $[\text{Co}(\text{gha})(\text{PH}_3)_2]^+$ and $[\text{Co}(\text{gha})]^+$

Calculations were first performed on a model system in which all phenyl groups in $[\text{Co}(\text{gha})(\text{PPh}_3)_2]^+$ were replaced with hydrogen atoms. The optimized structural parameters of the $[\text{Co}(\text{gha})(\text{PH}_3)_2]^+$ complex in closed shell singlet state are given in Table 2 along with the corresponding experimental values (atom labeling follows that in the crystal structure, see Fig. 1). It is seen that the calculated bond lengths are in reasonable agreement with the experimental values. Though the trends in C–C bond lengths are well described by the chosen level of theory, the Co–N and

Table 2 Experimental bond distances (Å) of octahedral $[\text{Co}(\text{gha})(\text{PPh}_3)_2]^+$ in comparison with the calculated values for the model systems $[\text{Co}(\text{gha})(\text{PH}_3)_2]^+$ and $[\text{Co}(\text{gha})]^+$

	$[\text{Co}(\text{gha})(\text{PPh}_3)_2]^+$ Expt.	$[\text{Co}(\text{gha})(\text{H}_3)_2]^+$ Calcd. RKS DFT	$[\text{Co}(\text{gha})]^+$ Calcd. RKS DFT	$[\text{Co}(\text{gha})]^+$ Calcd. BS-UKS DFT
Co(1)–N(1)	1.852(4)	1.881	1.823	1.842
Co(1)–N(2)	1.855(4)	1.881	1.823	1.842
Co(1)–O(1)	1.934(3)	1.967	1.871	1.867
Co(1)–O(2)	1.948(3)	1.967	1.871	1.867
Co(1)–P(1)	2.2737(15)	2.234	—	—
Co(1)–P(2)	2.3435(15)	2.234	—	—
O(1)–C(1)	1.314(6)	1.336	1.316	1.319
C(1)–C(2)	1.410(7)	1.418	1.420	1.420
C(2)–C(3)	1.364(7)	1.397	1.394	1.394
C(3)–C(4)	1.417(7)	1.422	1.430	1.429
C(4)–C(5)	1.379(7)	1.393	1.394	1.396
C(5)–C(6)	1.406(7)	1.418	1.414	1.413
C(1)–C(6)	1.414(7)	1.442	1.458	1.458
N(1)–C(6)	1.382(6)	1.387	1.376	1.379
N(1)–C(7)	1.306(5)	1.335	1.366	1.354
C(7)–C(8)	1.417(6)	1.428	1.396	1.409
N(2)–C(8)	1.321(6)	1.335	1.366	1.354
N(2)–C(9)	1.386(6)	1.387	1.376	1.379
C(9)–C(10)	1.393(7)	1.418	1.414	1.413
C(10)–C(11)	1.377(7)	1.393	1.394	1.396
C(11)–C(12)	1.395(7)	1.422	1.430	1.429
C(12)–C(13)	1.368(7)	1.396	1.394	1.394
C(13)–C(14)	1.410(7)	1.418	1.420	1.420
C(14)–C(9)	1.396(7)	1.442	1.458	1.458
O(2)–C(14)	1.333(5)	1.336	1.316	1.319

Co–O bond lengths are nevertheless both overestimated by 0.03 Å. The biggest discrepancies are observed for Co–P bond lengths which are predicted to be significantly shorter than the experimental values most likely due to the lesser steric bulk of the hydrogen atoms compared to the phenyl groups.

The stability of the singlet self consistent field (SCF) Kohn–Sham (KS) solution for the $[\text{Co}(\text{gha})(\text{PH}_3)_2]^+$ cation in its optimized geometry was tested with respect to triplet perturbations whose presence is indicative of singlet diradical character. The closed shell solution was found to be fully stable under all perturbations considered. However, the lowest energy Hessian eigenvalue is only 0.025 with a dominant (96%) contribution from the highest occupied molecular orbital (HOMO) to lowest unoccupied molecular orbital (LUMO) excitation. Since both of the active orbitals are in this case centered on the $(\text{gha})^{2-}$ ligand and have no contributions from the phosphine coligands, we decided to test what effect, if any, the removal of the PH_3 groups would have to the molecular structure as well as to the stability of the SCF KS solution. This is very informative considering the experimental results *i.e.* without coligands the synthetic approach failed to produce any crystalline products.

The optimized geometry of the truncated $[\text{Co}(\text{gha})]^+$ model system is given in Table 2. The calculated data set can be compared to the optimized structure of the full cation which shows that the cobalt–oxygen bond lengths are the structural parameters most significantly affected by the removal of the PH_3 groups and at 1.87 Å are much shorter than in the X-ray crystal structure despite the decrease of the coordination number from six to four in the calculated model. Interestingly, the closed shell singlet SCF KS solution for $[\text{Co}(\text{gha})]^+$ is unstable with respect to triplet perturbations as the lowest Hessian eigenvalue is negative, -0.070 (89% contribution from the HOMO–1 to LUMO excitation). This indicates that the removal of the phosphine coligands alters the electronic structure of the $(\text{gha})^{2-}$ ligand, changing its ground state from a closed shell singlet ($[\text{Co}(\text{gha})(\text{PH}_3)_2]^+$) to a singlet diradical ($[\text{Co}(\text{gha})]^+$).

The geometry optimization for $[\text{Co}(\text{gha})]^+$ was performed for a second time using a broken symmetry (BS) approach to account for the singlet diradical nature of the system; the calculated bond lengths are listed in Table 2. For the calculated geometry of BS $[\text{Co}(\text{gha})]^+$, the predicted distances within the ligand backbone are in good agreement in comparison to those found for the analogous closed shell structure. Most notably, the cobalt–nitrogen bond lengths are elongated by 0.02 Å with respect to RKS $[\text{Co}(\text{gha})]^+$ and are now in excellent agreement with the experimental values.

Electronic structures of the monocations $[\text{Co}(\text{gha})(\text{PH}_3)_2]^+$ and $[\text{Co}(\text{gha})]^+$

Since we used broken symmetry calculations in the remaining part of the computational work, we will adopt the following notation. The system is divided into two fragments and the notation BS(m , n) refers to a broken symmetry state with m unpaired spin-up electrons on fragment 1 and n unpaired spin-down electrons essentially localized on fragment 2. In most cases fragments 1 and 2 would correspond to the metal and the ligand, respectively. In our case, however, both the fragments 1 and 2 correspond to the diradical ligand. In general, the BS(m , n) notation refers to the initial guess of the symmetry of the KS determinant or a wave

function. Recently the BS approach has successfully been applied to analyze the bonding in transition metal complexes in the groups of Wieghardt–Neese³⁸ and others.³⁹

The BS(1,1) calculation for the truncated $[\text{Co}(\text{gha})]^+$ cation converged to the $M_s = 0$ solution indicating the presence of two antiferromagnetically coupled electrons in the ligand. The closed shell singlet state for the truncated model $[\text{Co}(\text{gha})]^+$ is higher in energy by 1.2 kcal mol⁻¹ compared to the BS(1,1) $M_s = 0$ state. The lowest energy triplet solution is energetically on par with the broken symmetry singlet and is found to be 2.0 kcal mol⁻¹ lower than the closed shell singlet state. Hence, at the BP86 level of theory, the ground state of the $[\text{Co}(\text{gha})]^+$ cation is a high-spin triplet which offers some explanation why the synthetic approach depicted in Scheme 3 was not successful without the introduction of coligands.

The electronic structure of the singlet $[\text{Co}(\text{gha})]^+$ cation can be examined in detail *via* analyzing the MOs of the broken symmetry KS solution. The square-planar structure features three predominantly metal-type d orbitals which are all doubly occupied and found in the spin-up as well in the spin-down manifold. This orbital occupation pattern defines a low-spin Co^{III} (d^6 , $S = 0$) configuration for the metal center. In addition, singly occupied ligand-based orbitals are identified which possess antiparallel spin orientation and give rise to the total spin density distribution depicted in Fig. 5. The analysis of the calculated Mulliken spin populations reveals that the spin density is polarized strictly in the ligand manifold (0.6 α -spin on one side and 0.6 β -spin on the other side of the ligand) and essentially no net spin density is localized on the central cobalt ion. Hence, this pattern sustains the representation of a singlet $[\text{Co}(\text{gha})]^+$ as a low-spin cobalt(III) coordinated to a singlet diradical dianionic gha ligand, resulting in an overall diamagnetic state.

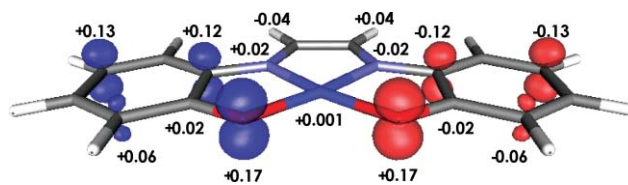


Fig. 5 Spin density plot of a square-planar monocation $[\text{Co}(\text{gha})]^+$ with calculated Mulliken spin density values derived from BS DFT calculations.

The broken symmetry KS solution for $[\text{Co}(\text{gha})]^+$ localizes spin density mostly on the two oxygen atoms. The stability analysis indicated that the active orbitals in the closed shell singlet determinant of $[\text{Co}(\text{gha})]^+$ are the HOMO–1 and LUMO which are depicted in Fig. 6. The HOMO–1 corresponds to cobalt d_{z^2} orbital (83%), whereas the LUMO is a linear combination of metal d_{xz} orbital (36%) with p_z orbitals of oxygen (11%), carbon (2–5%) and nitrogen (2%).

As expected, the shape of the LUMO resembles the spatial features in the spin density distribution calculated from the broken symmetry KS determinant (*cf.* Fig. 5). Considering the symmetry characteristics of the active orbitals, one expects that the HOMO–1 is (one of the MOs) able to mix with the frontier orbitals of the coligands when the two PH_3 groups bind to the square planar complex $[\text{Co}(\text{gha})]^+$. A fragment MO analysis conducted for $[\text{Co}(\text{gha})(\text{PH}_3)_2]^+$ confirms this notion. However, since the HOMO–1 of $[\text{Co}(\text{gha})]^+$ and the HOMO of PH_3 are both fully

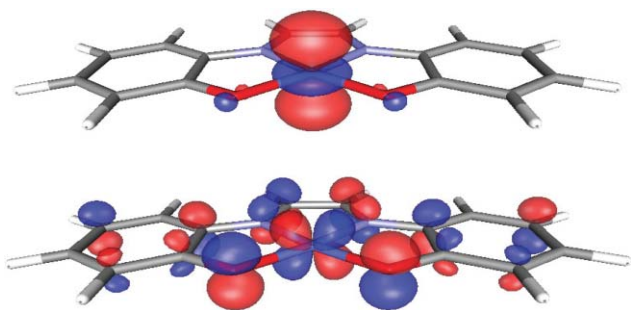


Fig. 6 HOMO-1 (top) and LUMO (bottom) of $[\text{Co}(\text{gha})]^+$ (isosurface value ± 0.05).

occupied in the respective fragments and their PCoP antibonding combination is unoccupied in $[\text{Co}(\text{gha})(\text{PH}_3)_2]^+$ (LUMO+1), some other linear combination of the initially unoccupied fragment orbitals needs to take electron density when the octahedral complex forms. Indeed, this orbital is found to be the HOMO of the full complex which corresponds to an almost pure LUMO (92%) of the $[\text{Co}(\text{gha})]^+$ fragment.

As elucidated above, the addition of two PH_3 (or, in general, PR_3) groups to $[\text{Co}(\text{gha})]^+$ causes significant changes in the orbital framework which leads to transfer of electron density to the LUMO of the metal-gha fragment. In essence, this effect, though mediated by the two PH_3 groups, is analogous to what takes place in the broken symmetry treatment of singlet state $[\text{Co}(\text{gha})]^+$. Hence, it can be readily understood why the full complex featuring an octahedral ligand field does not display SCF instability although the square planar truncated model is best viewed as containing a diradical ligand. We conclude this section by noting that despite the fact that the ground state of the $[\text{Co}(\text{gha})(\text{PH}_3)_2]^+$ cation can be described as a closed shell singlet,⁴⁰ the occupation of the LUMO of the $[\text{Co}(\text{gha})]^+$ fragment in $[\text{Co}(\text{gha})(\text{PH}_3)_2]^+$ leads to an electronic structure which is phenoxyl rather than phenolato-type.

Cyclic voltammetry

The electronic structure of compound **1** was assessed by performing cyclic voltammetry in dichloromethane solution at -10°C ; the experiments were performed in the scan rate variation from 0.05 to 1.60 V s^{-1} . There is one two electron oxidation and two one electron reductions discernible in the cyclic voltammogram of **1** (Fig. 7). It is seen that the second reduction at a more negative potential is irreversible at all scan rates and at $+0.200\text{ V}$ possesses a peak potential of $E_p = -0.88\text{ V}$ but the first reduction at $0.0\text{ V vs. Fc}^+/\text{Fc}$ is reversible at higher scan rates. The oxidation is almost irreversible at slow scans (0.05 V s^{-1}) and gains some reversibility at higher scan rates - in line with an interfering homogeneous follow-up reaction. At a scan rate of 0.80 or at 1.60 V s^{-1} the oxidation looks relatively reversible and one can evaluate a formal reduction potential of $E^\circ = +0.650\text{ V vs. Fc}^+/\text{Fc}$. Surprisingly, the reversibility of the oxidation did not improve much upon cooling the solution even to -30°C . Therefore, coulometric and EPR spectroscopic studies are not expected to deliver significant new information.

The peak current of oxidation was found to be about twice as high as that of reduction. The voltammogram was referenced to ferrocene which was oxidized at $+0.203\text{ V vs. the reference}$

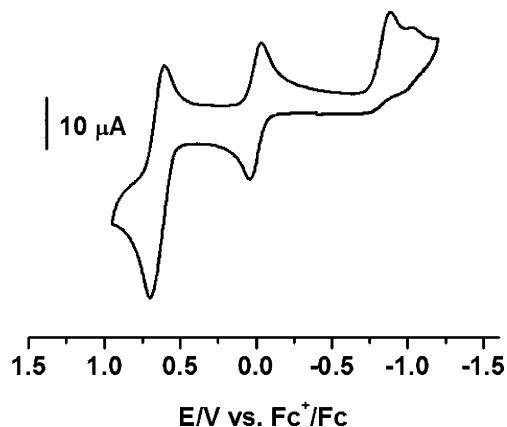
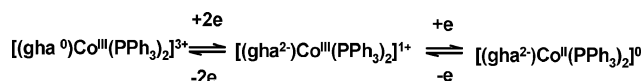


Fig. 7 Cyclic voltammogram of **1** in CH_2Cl_2 at the scan rate of 0.80 V s^{-1} at -10°C .

electrode. The measured data can be compared to the cyclic voltammograms measured for different metal complexes of the $(\text{gha})^{2-}$ ligand. However, only two studies, both conducted on ruthenium coordinated species, have been reported.²² We note that the difference between the first reduction and oxidation potentials in both cases is around 1.50 V . In the current case, the two electron oxidation at $+0.650\text{ V vs. Fc}^+/\text{Fc}$ and the second reduction at $-0.880\text{ V vs. Fc}^+/\text{Fc}$ are both assigned as gha centered (Scheme 4). The first reduction at $0.0\text{ V vs. Fc}^+/\text{Fc}$ is due to the $\text{Co}^{\text{III}}/\text{Co}^{\text{II}}$ couple; the reduction couple is very similar to that in the reported cobalt(salen) species with a similar coordination sphere.⁴¹



Scheme 4 Redox states of the complex and the ligand in **1**.

Conclusion

We reported the first single crystal X-ray structure of a glyoxalbis(2-hydroxyanil) (gha) coordinated to a transition metal ion in an unique complex salt $[\text{Co}^{\text{III}}(\text{gha})(\text{PPh}_3)_2][\text{Co}^{\text{II}}\text{Cl}_3(\text{PPh}_3)] \cdot \text{C}_2\text{H}_5\text{OH}$ (**1**). Complex **1** opens up an interesting opportunity to investigate the electronic properties of the redox active dianionic gha ligand which has eluded complete structural characterization for more than 50 years. Crystallographic bond parameters, spectral and magnetic properties as well as results from DFT calculations were collectively used to determine the ground state of the gha ligand in the cation of **1**. It was found that without the phosphine coligands, the Co-gha complex has a triplet ground state with the lowest energy singlet diradical state lying only 1 kcal mol^{-1} higher in energy. The introduction of phosphine groups alters the electronic structure of the square planar cation $[\text{Co}(\text{gha})]^+$ by transferring electron density from the metal to the atoms in the ligand framework. This gives rise to an overall closed shell singlet ground state which nevertheless retains phenoxyl-type electronic structure with some "radical character" as evidenced by the determined structural parameters and UV-Vis spectroscopic data for **1**. The possibility of the dianionic gha ligand to undergo intraligand redox chemistry represents an attractive feature. It would be interesting to see whether, with appropriate

metal atoms or coligands, it is possible to alter the electronic structure of the ligand so as to induce a diradical ground state. Work in this direction is in progress.

Acknowledgements

The present work was supported by the Council of Scientific and Industrial Research, CSIR (01(1957)/04/EMR-II), New Delhi, India. H.M.T acknowledges the Academy of Finland and the University of Jyväskylä for financial support.

References

- 1 M. Gomberg, *J. Am. Chem. Soc.*, 1900, **22**, 757.
- 2 (a) T. T. Tidwell, *Adv. Phys. Org. Chem.*, 2001, **36**, 1; (b) P. P. Power, *Chem. Rev.*, 2003, **103**, 789; (c) R. G. Hicks, *Org. Biomol. Chem.*, 2007, **5**, 1321.
- 3 (a) J. M. Rawson, A. J. Banister and I. Lavender, *Adv. Heterocycl. Chem.*, 1995, **62**, 137; (b) J. M. Rawson and G. D. McManus, *Coord. Chem. Rev.*, 1999, **189**, 135; (c) K. F. Preston and L. H. Sutcliffe, *Magn. Reson. Chem.*, 1990, **28**, 189; (d) P. Kaszynski, *J. Phys. Chem. A*, 2001, **105**, 7615; (e) P. Kaszynski, *J. Phys. Chem. A*, 2001, **105**, 7626; (f) R. T. Oakley, *Prog. Inorg. Chem.*, 1988, **36**, 299.
- 4 (a) R. Kuhn and H. Trischmann, *Angew. Chem., Int. Ed. Engl.*, 1963, **3**, 155; (b) E. C. Pare, D. J. R. Brook, A. Brieger, M. Badik and M. Schinke, *Org. Biomol. Chem.*, 2005, **3**, 4258; (c) F. A. Neugebauer, H. Fischer and R. Siegel, *Chem. Ber.*, 1988, **121**, 815.
- 5 (a) E. G. Rozantsev, *Free Nitroxyl Radicals*, Plenum, New York, 1970; (b) E. G. Rozantsev and V. D. Sholle, *Synthesis*, 1971, 401; (c) E. G. Rozantsev and V. D. Sholle, *Synthesis*, 1971, 190; (d) J. F. W. Keana, *Chem. Rev.*, 1978, **78**, 37.
- 6 C. Hawker, *Acc. Chem. Res.*, 1997, **30**, 373.
- 7 (a) R. A. Sheldon, *Acc. Chem. Res.*, 2002, **35**, 774; (b) B. Bar-On, Mohsen, R. Zhang, E. Feigin, M. Chevion and A. Samuni, *J. Am. Chem. Soc.*, 1999, **121**, 8070.
- 8 (a) *Magnetic Properties of Organic Materials*, ed. P. M. Lahti, Marcel Dekker, Inc., New York, 1999; (b) P. J. Low, *Dalton Trans.*, 2005, 2821; (c) M. T. Lemaire, *Pure Appl. Chem.*, 2004, **76**, 277.
- 9 (a) P. A. Frey, *Chem. Rev.*, 1990, **90**, 1343; (b) J. Stubbe and W. A. van der Donk, *Chem. Rev.*, 1998, **98**, 705; (c) R. H. Holms and E. I. Solomon, *Chem. Rev.*, 1996, **96**, 2239; (d) C. G. Pierpont and R. M. Buchanan, *Coord. Chem. Rev.*, 1981, **38**, 45; (e) Y. Wang, J. L. DuBois, B. Hedman, K. O. Hodgson and T. D. P. Stack, *Science*, 1998, **279**, 537.
- 10 C. G. Pierpont and C. W. Lange, *Prog. Inorg. Chem.*, 1994, **41**, 331.
- 11 H. Chun, C. N. Verani, P. Chaudhuri, E. Bothe, E. Bill, T. Weyhermüller and K. Wieghardt, *Inorg. Chem.*, 2001, **40**, 4157.
- 12 (a) K. Chlopek, E. Bill, T. Weyhermüller and K. Wieghardt, *Inorg. Chem.*, 2005, **44**, 7087; (b) O. Carugo, K. Djinovic, M. Rizzi and B. C. Castellani, *J. Chem. Soc., Dalton Trans.*, 1991, 1551; (c) D. Herebian, E. Bothe, F. Neese, T. Weyhermüller and K. Wieghardt, *J. Am. Chem. Soc.*, 2003, **125**, 9116; (d) D. Herebian, K. Wieghardt and F. Neese, *J. Am. Chem. Soc.*, 2003, **125**, 10997; (e) A. L. Balch and R. H. Holm, *J. Am. Chem. Soc.*, 1966, **88**, 5201; (f) P. Ghosh, A. Begum, D. Herebian, E. Bothe, P. Hildenbrand, T. Weyhermüller and K. Wieghardt, *Angew. Chem., Int. Ed.*, 2003, **42**, 563; (g) E. Bill, E. Bothe, P. Chaudhuri, K. Chlopek, D. Herebian, S. Kokatam, K. Ray, T. Weyhermüller, F. Neese and K. Wieghardt, *Chem.–Eur. J.*, 2005, **11**, 204; (h) C. N. Verani, S. Gallert, E. Bill, T. Weyhermüller, K. Wieghardt and P. Chaudhuri, *Chem. Commun.*, 1999, 1747; (i) H. Chun, C. N. Verani, P. Chaudhuri, E. Bothe, E. Bill, T. Weyhermüller and K. Wieghardt, *Inorg. Chem.*, 2001, **40**, 4157.
- 13 P. Ghosh, E. Bill, T. Weyhermüller and K. Wieghardt, *J. Am. Chem. Soc.*, 2003, **125**, 3967.
- 14 P. Chaudhuri and K. Wieghardt, *Prog. Inorg. Chem.*, 2001, **50**, 151.
- 15 F. N. Penkert, T. Weyhermüller, E. Bill, P. Hildebrandt, S. Lecomte and K. Wieghardt, *J. Am. Chem. Soc.*, 2000, **122**, 9663.
- 16 T. Buttner, J. Geier, G. Frison, J. Harmer, C. Calle, A. Schweiger, H. Schonberg and H. Grutzmacher, *Science*, 2005, **307**, 235.
- 17 S. Kimura, E. Bill, E. Bothe, T. Weyhermüller and K. Wieghardt, *J. Am. Chem. Soc.*, 2001, **123**, 6025.
- 18 (a) M. Shivakumar, K. Pramanik, P. Ghosh and A. Chakravorty, *Inorg. Chem.*, 1998, **37**, 5968; (b) M. Shivakumar, K. Pramanik, P. Ghosh and A. Chakravorty, *Chem. Commun.*, 1998, 2103; (c) K. Pramanik, M. Shivakumar, P. Ghosh and A. Chakravorty, *Inorg. Chem.*, 2000, **39**, 195; (d) M. Schwach, H. D. Hausen and W. Kaim, *Inorg. Chem.*, 1999, **38**, 2242; (e) N. Doslik, T. Sixt and W. Kaim, *Angew. Chem., Int. Ed. Engl.*, 1998, **37**, 2403.
- 19 P. Ghosh, E. Bill, E. Bothe, T. Weyhermüller, F. Neese and K. Wieghardt, *J. Am. Chem. Soc.*, 2003, **125**, 1293.
- 20 (a) E. Bayer, *Angew. Chem.*, 1957, **69**, 107; (b) E. Bayer, *Angew. Chem.*, 1959, **71**, 426; (c) E. Bayer, *Chem. Ber.*, 1957, **90**, 2325; (d) E. Bayer, *Chem. Ber.*, 1957, **90**, 2785; (e) E. Bayer and G. Schenk, *Chem. Ber.*, 1960, **93**, 1184; (f) E. Bayer, *Angew. Chem., Int. Ed. Engl.*, 1964, **3**, 325.
- 21 (a) G. Bandoli and D. A. Clemente, *J. Chem. Soc., Dalton Trans.*, 1975, 612; (b) R. Benedix, F. Dietz and H. Hennig, *Inorg. Chim. Acta*, 1988, **147**, 179; (c) G. Bandoli, L. Cattalini, D. A. Clemente, M. Vidali and P. A. Vigado, *J. Chem. Soc., Chem. Commun.*, 1972, 344; (d) T. Majima and Y. Kawasaki, *Bull. Chem. Soc. Jpn.*, 1978, **51**, 1893.
- 22 (a) S. Kar, B. Ghumaan, F. A. Urbanos, J. Fiedler, R. B. Sunoj, R. Jimenez-Aparico, W. Kaim and G. K. Lahiri, *Inorg. Chem.*, 2005, **44**, 8715; (b) S. Kar, B. Sarkar, S. Ghumaan, M. Leboschka, J. Fiedler, W. Kaim and G. K. Lahiri, *Dalton Trans.*, 2007, 1934.
- 23 (a) H. Jadamus, Q. Fernando and H. Freiser, *J. Am. Chem. Soc.*, 1964, **86**, 3056; (b) I. Murase, *Bull. Chem. Soc. Jpn.*, 1959, **32**, 827; (c) E. Bayer, *Angew. Chem.*, 1961, **73**, 659.
- 24 SAINT+, Version 6.02, Bruker-AXS, Madison, WI, 1999.
- 25 G. M. Sheldrick, *SADABS, Version 2.00*, University of Göttingen, Göttingen, Germany, 2002.
- 26 G. M. Sheldrick, *SHELXL-97, Program for refinement of crystal structures*, University of Göttingen, Germany, 1997.
- 27 (a) F. Neese, *ORCA: An ab initio, Density Functional and Semiempirical Electronic Structure Program Package, Version 2.4, Revision 36*, Max-Planck Institut für Bioorganische Chemie, Mülheim/Ruhr, Germany, 2005; (b) *TURBOMOLE, Program Package for ab initio Electronic Structure Calculations, Version 5.9.1*, Theoretical Chemistry Group, University of Karlsruhe, Karlsruhe, Germany, 2007; (c) R. Ahlrichs, M. Bär, M. Häser, H. Horn and C. Kölmel, *Chem. Phys. Lett.*, 1989, **162**, 165.
- 28 (a) A. D. Becke, *J. Chem. Phys.*, 1993, **98**, 5648; (b) A. D. Becke, *J. Chem. Phys.*, 1986, **84**, 4524; (c) C. T. Lee, W. T. Yang and R. G. Parr, *Phys. Rev. B*, 1988, **37**, 785.
- 29 (a) A. Schäfer, H. Horn and R. Ahlrichs, *J. Chem. Phys.*, 1992, **97**, 2571; (b) A. Schäfer, C. Huber and R. Ahlrichs, *J. Chem. Phys.*, 1994, **100**, 5829.
- 30 *ADF2006.01, SCM, Theoretical Chemistry*, Vrije Universiteit, Amsterdam, Netherlands, <http://www.scm.com>.
- 31 (a) L. J. Laaksonen, *Mol. Graph.*, 1992, **10**, 33; (b) D. L. Bergman, L. Laaksonen and A. Laaksonen, *J. Mol. Graphics Modell.*, 1997, **15**, 301.
- 32 M. G. Gardiner, G. R. Hanson, M. J. Henderson, F. C. Lee and L. C. Raston, *Inorg. Chem.*, 1994, **33**, 2456.
- 33 T. Glaser, M. Heidemeier and T. Lügger, *J. Chem. Soc., Dalton Trans.*, 2003, 2381.
- 34 (a) A. Sokolowski, B. Adam, T. Weyhermüller, K. Hildenbrand, R. Schnepf, P. Hildebrandt, E. Bill and K. Wieghardt, *Inorg. Chem.*, 1997, **36**, 3702; (b) J. Muller, A. Kikuchi, E. Bill, T. Weyhermüller, P. Hildebrandt, L. Ould-Moussa and K. Wieghardt, *Inorg. Chim. Acta*, 2000, **297**, 265.
- 35 A. Sokolowski, E. Bothe, E. Bill, T. Weyhermüller and K. Wieghardt, *Chem. Commun.*, 1996, 1671.
- 36 (a) B. Adam, E. Bill, E. Bothe, B. Goerdts, G. Haselhorst, K. Hildenbrand, A. Sokolowski, S. Steenken, T. Weyhermüller and Karl Wieghardt, *Chem.–Eur. J.*, 1997, **3**, 308; (b) M. D. Snodin, L. Ould-Moussa, U. Wallmann, S. Lecomte, V. Bachler, E. Bill, H. Hummel, T. Weyhermüller, P. Hildebrandt and K. Wieghardt, *Chem.–Eur. J.*, 1999, **5**, 2554.
- 37 (a) J. G. Radziszewski, M. Gill, A. Gorski, J. Spanget-Larsen, J. Waluk and B. J. Mroz, *J. Chem. Phys.*, 2001, **115**, 9733; (b) C. Adamo, R. Subra, A. D. Matteo and V. Barone, *J. Chem. Phys.*, 1998, **109**, 10244.
- 38 (a) V. Bachler, G. Olbrich, F. Neese and K. Wieghardt, *Inorg. Chem.*, 2002, **41**, 4179; (b) S. Blanchard, F. Neese, E. Bothe, E. Bill, T. Weyhermüller and K. Wieghardt, *Inorg. Chem.*, 2005, **44**, 3636; (c) D.

-
- Herebian, E. Bothe, F. Neese, T. Weyhermüller and K. Wieghardt, *J. Am. Chem. Soc.*, 2003, **125**, 9116; (d) D. Herebian, K. Wieghardt and F. Neese, *J. Am. Chem. Soc.*, 2003, **125**, 10997; (e) L. D. Slep, A. Mijovilovich, W. Meyer-Klaucke, T. Weyhermüller, E. Bill, E. Bothe, F. Neese and K. Wieghardt, *J. Am. Chem. Soc.*, 2003, **125**, 15554.
- 39 (a) C. Remenyi and M. Kaupp, *J. Am. Chem. Soc.*, 2005, **127**, 11399; (b) A. Bencini, C. Carbonera, A. Dei and M. G. F. Vaz, *J. Chem. Soc., Dalton Trans.*, 2003, 1701; (c) L. Noodleman, C. Y. Peng, D. A. Case and J. M. Mouesca, *Coord. Chem. Rev.*, 1995, **144**, 199.
- 40 Strictly speaking, the KS determinant is not a real wave function but describes a hypothetical reference state. The existence of a symmetry-broken singlet UKS determinant that is lower in energy than the corresponding RKS solution can nevertheless be used as a qualitative indicator of diradical character. However, the wave function can have an internal instability even if all eigenvalues in the KS SCF stability analysis are found to be positive.
- 41 H. Shimakoshi, W. Ninomiya and Y. Hisaeda, *J. Chem. Soc., Dalton Trans.*, 2001, 1971.